Highlights of Spanish Astrophysics XII, Proceedings of the XVI Scientific Meeting of the Spanish Astronomical Society held on July 15 - 19, 2024, in Granada, Spain. M. Manteiga, F. González Galindo, A. Labiano Ortega, M. Martínez González, N. Rea, M. Romero Gómez, A. Ulla Miguel, G. Yepes, C. Rodríguez López, A. Gómez García and C. Dafonte (eds.), 2025

Multi-species modelling of M1-92: the death of a star told by its isotopic ratios

Masa, E.[1], Alcolea, J.[1], Santander-García, M.[1] Bujarrabal, V.[2], Sánchez Contreras, C.[3] and Castro-Carrizo, A.[4]

[1] Observatorio Astronómico Nacional (IGN), Alfonso XII 3, E-28014 Madrid, Spain
[2] Observatorio Astronómico Nacional (IGN), Ap 112, E-28803 Alcalá de Henares, Spain
[3] Centro de Astrobiología (CSIC-INTA), Camino Bajo del Castillo s/n, E-28691 Villanueva de la Cañada, Spain
[4] Institute de Radioastronomie Millimetrique, rue de la Piscine 300, F-38406 St. Martin d'Heres, France

Abstract

Ongoing improvements in sub-mm- and mm-range instrumentation allows the study with more detail and precision of nebulae around post-AGB stars, termed pre-planetary nebulae, including the use of molecular tracers other than CO in its various isotopic substitutions. Using an updated version of the modelling tool SHAPE+shapemol, we can now create morpho-kinematical models to reproduce observations of these shells in up to 10 different molecular species, allowing an accurate description of their physical features as well as their molecular abundances and isotopic ratios.

The pre-planetary nebula M1-92 (Minkowski's Footprint) is one of the most iconic objects of its kind, with a wide range of physical conditions and more than 20 molecular species detected. We model this nebula, reproducing the observational data from IRAM-30m spectra and NOEMA interferometric maps, trying to understand the unusual evolution of its central star in the last phases of its life.

The results show interesting features that tell us M1−92's death story. The low-density and high-temperature areas of turbulent gas found across the nebula's symmetry axis suggest a periodic mass ejection that could still be happening. A measured $^{17}O/^{18}O$ isotopic ratio of 1.6 indicates that the central star should have turned C-rich by the end of the AGB, as opposed to its O-rich nebula. This suggests that M1-92 resulted from a sudden massive ejection event, which also interrupted the AGB evolution of the central source, preventing its transformation into a C-rich star. We also detect different ratios of $^{12}C/^{13}C$ across the nebula, which is particularly relevant in the inner equatorial region traced by HCO^+ and $H^{13}CO^+$, indicating an isotopic ratio change during the post-AGB evolution.

1 Introduction

The wide variety of shapes and symmetries found in planetary nebulae (PNe) is one of the aspects of stellar evolution that still defies our comprehension. Several mechanisms have been proposed to explain the processes that reshape the isotropic circumstellar envelopes (CSEs) of asymptotic giant branch (AGB) stars into bipolar or multi-polar PNe [1, 2]. Most of them require the presence of a companion to provide the angular momentum that results in an ejection through a preferential axis [3].

Pre-planetary nebulae (pPNe), the transitional objects in between AGB CSEs and PNe, are privileged sources of information on this transformation. Minkowsky's Footprint, pPN M1−92, is one of the most iconic and interesting nebulae in this context. Located at a distance of 2.5 kpc around a B-type post-AGB star, it shows a bipolar shape $11''\times6''$ in size [4]. Previous mapping of the ^{13}CO J=2−1 line emission at 0.5 arc-sec resolution showed that the main nebular structure has a constant radial velocity gradient of 7.4 km s^{-1} per arc-sec [1]. The nebula, as shown in those previous maps, consists of two emptied lobes, divided by an equatorial denser structure, ending in two axial tips. All these components show a homologous expansion with a kinematical age of 1200 yr. This suggests that M1−92 resulted from a brief mass-loss event amounting to $\sim 0.9\,M_\odot$ in less than 100 yr, resulting in a mass loss rate larger than $10^{-2}\,M_\odot$ yr^{-1}[5]. This imposes strong constraints to the mechanism powering these ejections and the shaping of the nebula, in line with those provided by common envelope ejection models [6].

In addition, two compact regions inside the lobes, the knots, have been revealed by the emission from optical atomic forbidden lines and vibrationally excited H_2, and are thought to contain shocked gas [7, 8]. These areas present younger kinematic ages (about 650 yr) than the main shell traced by CO [9].

This object also presents interesting chemistry and elemental isotopic ratios. It has more than 20 molecular species detected by single dish observations, including all CO stable isotopomers, HCN, H^{13}CN, HCO$^+$, and H^{13}CO$^+$[10]. Isotopic ratios for ^{12}C/^{13}C as well as ^{17}O/^{18}O have been studied, suggesting that despite the O-rich nature of the nebula, the central AGB star should have turned C-rich, had the sudden mass-loss event occurred later [11, 12, 5], or followed the usual evolution of AGB stars under the assumption of solar-like metallicity.

2 Data and model

To model M1−92 we used `SHAPE`, a free software that allows 3-D modelling and simulation of the emission of extended, gaseous astrophysical objects [13]. The emission from molecular lines is computed through `shapemol`, a built-in plugin that was limited to ^{12}CO and ^{13}CO[14], but we have expanded to C^{17}O, C^{18}O, HCO$^+$, and H^{13}CO$^+$as part of this project. The basis of these computations is the LVG-approximation treatment of the non-LTE excitation of the species [15], with an exact solution for the radiative transfer and simulation of the emerging line emission as observed either with single dishes or interferometers. Further details on these

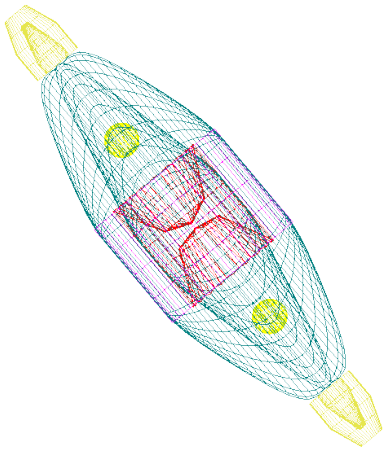

Figure 1: Wired representation of the best-fit model based on available data of the molecular envelope of the pPN M1-92 showing its structures. The observer's point of view from Earth is located to its left. Green: The main shell, which forms the walls of the empty lobes and mainly consists of cold gas. Soft yellow: Tips structure composed of an inner layer of low-density warm gas and an outer layer with very similar conditions to the main shell. Red: Equatorial structure with high density, defining the lobes' base. Purple: Ring around the central cylinder with the same physical properties as the main shell. Bright yellow: Knots inside the empty lobes where ionised gas has been found.

computations will be discussed in Masa et al. (in prep.).

The observational data we aim to reproduce with our model comes from six species: ^{12}CO, ^{13}CO, C^{17}O, C^{18}O, HCO$^+$ and H^{13}CO$^+$. In total, 17 line profiles and 5 interferometric maps were reproduced by our model. We work with single-dish data from ^{12}CO (lines J=1−0, J=2−1, J=5−4, J=7−6 and J=9−8), ^{13}CO, C^{17}O, C^{18}O (lines J=1−0 and J=2−1 for each), HCO$^+$, and H^{13}CO$^+$ (J=1−0, J=2−1 and J=3−2 for each). In addition, the four species with interferometric data are ^{13}CO, C^{17}O, C^{18}O, and HCO$^+$, all of them mapped in the J=2−1 line. All maps come from IRAM's interferometer NOEMA, while most of the single-dish lines come from IRAM-30m, except for the ^{12}CO J=5−4, J=7−6 and J=9−8 lines that were obtained through Herschel Space Observatory (HSO) HiFi observations.

The best-fit model is shown in Fig. 1, where each of the structures previously described are represented. In some cases, like the polar tips or the equatorial region, a two-layered structure had to be incorporated to accurately reproduce the observational data.

This best-fit model is rendered with a resolution of 127 × 127 cells in a 40″× 40″ window, using the observed sizes for the nebula and a beam the same size of observations for each spectral line. In addition, the resulting maps from the model are put through the same interferometric process (uv-filtering, uv-mapping and cleaning) as that of real observations. Finally, our model is considered finished only when it is able to simultaneously reproduce the observational data with changes between different species owing only to their different abundances with respect to H_2.

3 Results

With the interferometric maps in CO isotopes, we can reproduce the geometry and physical distribution of the gas. In Fig. 2 we present the comparison side by side between the observational data of the ^{13}CO map and our model reproduction, together with the resulting residuals. In particular, these images consist of P-V diagrams, that due to the linear velocity law ($v \propto r$), we can use as representative cuts of the nebula, since the observed velocity will always be proportional to the position along the line of sight in structures following this law.

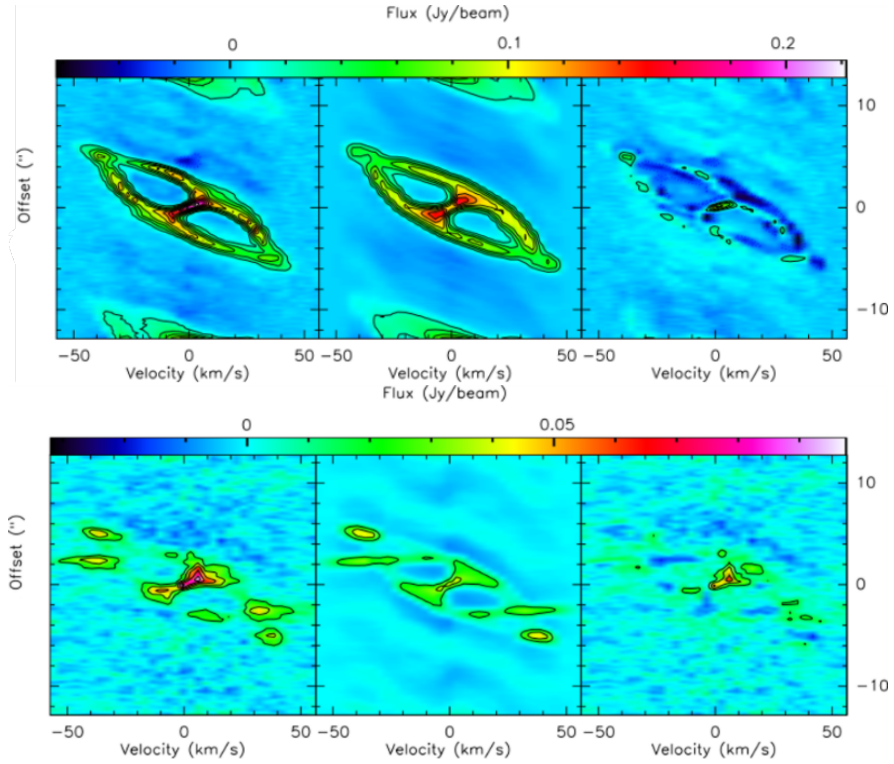

Figure 2: P-V diagrams along the nebular symmetry axis for ^{13}CO (top) and HCO$^+$ (bottom) J=2−1 transition. Observational data is shown on the left, model reproduction on the central panel and observation–model residuals on the right.

In the central image showing the reproduction from our model, we can identify features resulting from the instrumental processing of the observations due to uneven and incomplete coverage of the *uv*-plane. Some of these features are the artefact emission around the spatial axis, as well as certain asymmetries across the nebula that are not present in our perfectly symmetrical model, like the narrower parts close to the polar tips or a slightly wavy texture on the external surface of the shell.

Finally, observing the resulting fluxes in the residues image, we can conclude that our model is a very accurate description of the molecule-rich nebula except for a bright spot found on the central part of the nebula, slightly displaced towards positive velocities.

Despite not being mapped in any CO species, the wide range of energies covered by the observational profiles shows an evolution from a block emission in the low-J lines to a three-peak distribution. This can only be reproduced by adding a second layer of warmer gas inside the polar tips and with the presence of CO in the knots previously detected in the optical/NIR bands. Therefore, the lack of these structures in the CO maps is not due to the lack of CO species in the ionised knots, but because of the low excitation gas preferentially traced by the mapped low-J transitions.

For a reliable study of these inner structures, we need to reproduce the HCO^+ map. As seen in Fig. 2 the emission from the knots shows a wide velocity dispersion and a distribution fairly reproduced by a velocity field typical of shock fronts. Once again, the residuals panel shows an excellent fit obtained by our model, except for the bright spot on the central region, again clearly displaced towards positive velocities.

Following this process for all the observational data collected, we derive a specific value for the abundance relative to H_2 for each species, which allows us to obtain the isotopic ratios:

- $^{12}CO/^{13}CO/C^{17}O/C^{18}O = 1/30/550/880$
- $C^{17}O/C^{18}O = 1.6$
- $HCO^+/H^{13}CO^+ = 10$

These ratios are the consequence of the adjustments needed in the relative abundance to reproduce the observational data by our model, but they match those obtained directly by line ratios after applying frequency and Einstein coefficient corrections in the case of the optically thin species.

4 Discussion and conclusion

The analysis of CO data and the derived relative abundances for $C^{17}O$ and $C^{18}O$ confirm a $^{17}O/^{18}O$ ratio of 1.6. Assuming a solar metallicity for the central star, which is a reasonable assumption given its location in the disk of our galaxy (galactic declination $\sim 4°$), this ratio corresponds to an initial mass for the central AGB star of around 1.7 $M_\odot$ [16, 17, 18]. This mass should have been enough for the star to have experienced a number of third dredge up (TDU) events enough to become C-rich.. The combination of this isotopic ratio information with the nebular age of 1200 yr from the kinematics for most of the mass, makes it evident that a common envelope ejection or a sudden event of similar characteristics is a must when explaining the origin and shaping of this nebula. This event, with such a huge mass ejection, would have been enough to interrupt the normal AGB evolution of the star, preventing it from becoming C-rich and resulting in the final mixed chemistry we find on the nebula, thus providing a natural explanation for all the data gathered so far.

When analysing the results from our model we also find a discrepancy in the $^{12}C/^{13}C$ isotopic ratio, depending on whether we estimate it from $^{12}CO/^{13}CO$ or from $H^{12}CO^+/H^{13}CO^+$. Despite this seemingly contradictory result, it is important to notice that CO and HCO^+ trace different regions with different conditions. While CO is dominated by the emission of dense

and cold gas, especially the low-J lines, which are the ones used to derive isotopic ratios, HCO^+ trace the regions with active shocks, turbulent and with much higher temperatures despite their lower density. This suggests that the $^{12}CO/^{13}CO$ ratio must have experienced changes during the last 1200 yr. Further investigation is required to elucidate the origin of these isotopic ration changes.

A deeper analysis of the nebula's properties can be found in [19]. Derived magnitudes and their resulting discussion are expected to be found in Masa et al. (in prep.).

Acknowledgments

This research is part of the I + D + i projects PID2019-105203GB-C21 and PID2019-105203GB-C22 founded by Spanish AEI (MICIU) grant 10.13039/501100011033.

References

[1] Alcolea, J., Neri, R., Bujarrabal, V., 2007, A&A, 468, L41–L44

[2] Jones, D., Boffin, H.M.J., 2017, Nat. Astron., 1, 0117

[3] Douchin, D., De Marco, O., Frew, D.J., Jacoby, G.H., Jasniewicz, G., Fitzgerald, M., Passy, J.C., Harmer, D., Hillwig, T., Moe, M., 2015, MNRAS, 448, 3132–3155

[4] Sánchez Contreras, C., Sahai, R., Gil de Paz, A., Goodrich, R., 2008, ApJ Suppl. Ser., 179, 166-194

[5] Bujarrabal, V., Alcolea, J., Neri, R., 1998, ApJ, 504, 915–920

[6] Ohlmann, S.T., Röpke, F.K., Pakmor, R., Springel, V., 2016, ApJ Lett., 816, L9

[7] Solf, J. 1994, A&A, 282, 567–585

[8] Bujarrabal, V., Alcolea, J., Sahai, R., Zamorano, J., Zijlstra, A.A., 1998, A&A, 331, 361–371

[9] Davis, C.J., Smith, M.D., Gledhill, T.M., Varricatt, W.P., 2005, MNRAS, 360, 104–118

[10] Alcolea, J., Agúndez, M., Bujarrabal, V., Castro-Carrizo, A., Desmurs, J.F., Sánchez Contreras, C., Santander-García, M., 2018, Proc. IAU, 343, 343–344

[11] Alcolea, J., Agúndez, M., Bujarrabal, V., Castro-Carrizo, A., Desmurs, J.F., Martínez-Fernández, J.E., Sánchez Contreras, C., Santander-García, M., 2022, Galaxies,10, 47

[12] Bujarrabal, V., Alcolea, J., Neri, R., Grewing, M., 1997, A&A, 320, 540–552

[13] Steffen, W., Koning, N., Wenger, S., Morisset, C., Magnor, M., 2011, IEEE Trans. Vis. Comput. Graph., 17, 454–465

[14] Santander-García, M., Bujarrabal, V., Koning, N., Steffen, W., 2015, A&A, 573, A56

[15] Castor, J.I., 1970, MNRAS, 149, 111

[16] Karakas, A.I, 2014, MNRAS, 445, 347–358

[17] Cristallo, S., Piersanti, L., Straniero, O., Gallino, R., Domínguez, I., Abia, C., Di Rico, G., Quintini, M., Bisterzo, S., 2011, ApJ Suppl. Ser., 197, 17

[18] Stancliffe, R.J., Tout, C.A., Pols, O.R., 2004, MNRAS, 352, 984–992

[19] Masa, E., Alcolea, J., Santander-García, M., Bujarrabal, V., Sánchez Contreras, C., Castro-Carrizo, A., 2024, Galaxies, 12(5), 63